

**Phonon softening in  $\text{Lu}(\text{Pt}_{1-x}\text{Pd}_x)_2\text{In}$  close to a zero-temperature structural instability**T. Gruner<sup>1,2</sup>, S. Lucas,<sup>1</sup> C. Geibel,<sup>1</sup> K. Kaneko,<sup>3</sup> S. Tsutsui,<sup>4,5</sup> K. Schmalzl,<sup>6</sup> and O. Stockert<sup>1,\*</sup><sup>1</sup>Max-Planck-Institut für Chemische Physik fester Stoffe, 01187 Dresden, Germany<sup>2</sup>Cavendish Laboratory, University of Cambridge, Cambridge CB3 0HE, United Kingdom<sup>3</sup>Materials Sciences Research Center, Japan Atomic Energy Agency, Tokai, Naka, Ibaraki 319-1195, Japan<sup>4</sup>Japan Synchrotron Radiation Research Institute, SPring-8, Sayo, Hyogo 679-5198, Japan<sup>5</sup>Institute of Quantum Beam Science, Graduate School of Science and Engineering, Ibaraki University, Hitachi, Ibaraki 316-8511, Japan<sup>6</sup>Jülich Centre for Neutron Science JCNS, Forschungszentrum Jülich GmbH, Outstation at ILL, 38042 Grenoble, France

(Received 15 August 2022; accepted 9 September 2022; published 23 September 2022)

The disappearance of a charge-density-wave (CDW) transition in  $\text{Lu}(\text{Pt}_{1-x}\text{Pd}_x)_2\text{In}$  is thought to be closely linked to a maximum of the superconducting transition temperature in the system. We studied the superstructure and the phonon softening in  $\text{Lu}(\text{Pt}_{0.5}\text{Pd}_{0.5})_2\text{In}$  by means of neutron and high-resolution inelastic x-ray scattering. A full phonon softening at  $q_{\text{CDW}} = (0.50, 0.50)$  with the appearance of superstructure peaks could be clearly identified. This supports the CDW transition to be a continuous transition. The large tail of the superstructure intensity above the CDW transition indicates the importance of critical fluctuations. In general, the observed phonon dispersion relations are quite similar to those predicted by theoretical calculations. However, the softening occurs in a much narrower momentum range than predicted.

DOI: [10.1103/PhysRevB.106.115142](https://doi.org/10.1103/PhysRevB.106.115142)**I. INTRODUCTION**

The investigation of quantum critical points (QCPs), i.e., continuous phase transitions occurring at absolute zero temperature, is one of the most exciting research topics in current condensed-matter physics [1–5]. Systems are tuned by nonthermal control parameters to approach a QCP, e.g., magnetic field or chemical composition. Exotic phenomena, such as superconductivity, metamagnetism, and non-Fermi-liquid behavior are often observed in the vicinity of a QCP. Here, critical order-parameter fluctuations are crucial for the evolution of the exotic phases and unconventional behavior in physical properties. Up to now, quantum criticality has been mainly investigated in magnetic systems, but recently first materials were discovered, which exhibit a structural or charge-density-wave QCP (in metals a displacive, structural transition is accompanied by a CDW transition [6]). In such compounds, a softening of relevant phonons and related fluctuations of the crystal structure drive the quantum phase transition.

Phonon softening at structural phase transitions has been studied for quite a long time. Most prominently  $\text{SrTiO}_3$  has been investigated in great detail by inelastic neutron scattering and important results on the phonons in the compound were

obtained [7,8]. Other compounds include  $\text{KMnF}_3$ ,  $\text{KTaO}_3$ , or  $\text{PbTiO}_3$  to mention just a few. However, these studies focused on finite-temperature structural phase transitions [7,8]. Only recently a few compounds have been reported to exhibit a structural QCP, most notably  $(\text{Ca}_x\text{Sr}_{1-x})_3\text{Ir}_4\text{Sn}_{13}$  [9,10],  $(\text{Ca}_x\text{Sr}_{1-x})_3\text{Rh}_4\text{Sn}_{13}$  [10–12], and  $\text{Lu}(\text{Pt}_{1-x}\text{Pd}_x)_2\text{In}$  [13].

The alloying series  $\text{Lu}(\text{Pt}_{1-x}\text{Pd}_x)_2\text{In}$  appears to be a model system to study a structural QCP [13]. In the parent compound  $\text{LuPt}_2\text{In}$ , a Peierls transition from a face-centered-cubic Heusler structure towards a body-centered-cubic superstructure occurs at  $T_{\text{CDW}} = 490$  K by a doubling of the lattice parameters along all principal directions [13,14].  $\text{LuPt}_2\text{In}$  remains nonmagnetic at all temperatures with superconductivity showing up at temperatures below  $T_c = 0.4$  K. By substituting Pd for Pt, the structural transition in  $\text{Lu}(\text{Pt}_{1-x}\text{Pd}_x)_2\text{In}$  is linearly suppressed to zero temperature with a critical Pd content of  $x_c \approx 0.58$  [13]. Around the structural instability, i.e., at  $T_{\text{CDW}} = 0$ , the superconductivity in the system is strongly enhanced with a maximum superconducting  $T_c = 1.1$  K. Interestingly, recent results on the basis of *ab initio* density functional theory (DFT) propose that  $T_{\text{CDW}}$  in  $\text{Lu}(\text{Pt}_{1-x}\text{Pd}_x)_2\text{In}$  can be tuned by hydrostatic pressure, too [15]. This prediction was verified by experimental high-pressure data taken on poly- and single-crystalline samples [16,17]. Furthermore, these measurements revealed a direct impact of pressure as external tuning parameter on  $T_c$ . All this suggests a direct relation between superconductivity and the low-energy lattice dynamics at the  $T = 0$  structural instability. So far the low-energy phonons have mainly been studied indirectly through heat-capacity measurements [13]. As obtained from fits to the heat capacity,  $C = \gamma T + \beta T^3$  ( $\gamma$  being the Sommerfeld coefficient), the phononic contri-

\*oliver.stockert@cpfs.mpg.de

bution  $\beta$  to the heat capacity at low temperatures  $T$  displays a pronounced maximum around the critical Pd concentration  $x_c$ . Neutron scattering performed on powder of pure  $\text{LuPt}_2\text{In}$  gave indications for a softening of some phonon modes around  $T_{\text{CDW}} \approx 490$  K and could detect the appearance of a superstructure peak below  $T_{\text{CDW}}$  [13]. Very recent x-ray diffraction on  $\text{Lu}(\text{Pt}_{1-x}\text{Pd}_x)_2\text{In}$  powder with  $x = 0.3, 0.4$ , and  $0.5$  revealed superstructure peaks being indexed by a propagation vector  $\mathbf{q}_{\text{CDW}} = (0.5, 0.5, 0)$  [18]. However, detailed information of the low-energy phonons and their softening in  $\text{Lu}(\text{Pt}_{1-x}\text{Pd}_x)_2\text{In}$  is highly desired. Here, we report on a combined inelastic neutron and high-resolution inelastic x-ray scattering experiment on  $\text{Lu}(\text{Pt}_{1-x}\text{Pd}_x)_2\text{In}$  single crystals to study the low-energy phonons in the system with a particular focus on the phonon softening at  $T_{\text{CDW}}$ .

## II. EXPERIMENTAL DETAILS

Single crystals of  $\text{Lu}(\text{Pt}_{1-x}\text{Pd}_x)_2\text{In}$  were grown by Bridgman technique and oriented by x-ray Laue backscattering as described elsewhere [17]. Powderized pieces of the crystals were checked by x-ray powder diffraction. We performed inelastic neutron scattering as well as high-resolution inelastic x-ray scattering. The neutron-scattering experiment was carried out on the thermal triple-axis spectrometer IN3 located at the high-flux reactor of the Institut Laue-Langevin in Grenoble/France. The spectrometer was operated with horizontal collimation just before and after the sample (open-40'-40'-open) and a fixed final neutron energy of  $E_f = 14.7$  meV (fixed  $k_f = 2.66 \text{ \AA}^{-1}$ ) giving an energy resolution of about  $0.8$  meV (FWHM, full width at half maximum) at zero energy transfer. The crystal was mounted with the [001] axis vertical yielding a  $(hk0)$  horizontal scattering plane. Data were collected on a  $\text{Lu}(\text{Pt}_{0.6}\text{Pd}_{0.4})_2\text{In}$  single crystal around the  $(2.5, 1.5, 0)$  superstructure position (in the notation of the high-temperature Heusler structure) at room temperature for energy transfers up to  $8.4$  meV. Typical counting times were  $2$  min per point. We also measured the low-energy phonons in  $\text{Lu}(\text{Pt}_{0.5}\text{Pd}_{0.5})_2\text{In}$  and in  $\text{Lu}(\text{Pt}_{0.2}\text{Pd}_{0.8})_2\text{In}$  on the high-resolution inelastic x-ray spectrometer BL35XU at the SPring-8 synchrotron in Hyogo/Japan. For our measurements BL35XU was used with a Si (11 11 11) backscattering monochromator giving an energy resolution of  $\approx 1.4$  meV. The  $\text{Lu}(\text{Pt}_{1-x}\text{Pd}_x)_2\text{In}$  single crystals were attached to the cold head of a closed-cycle refrigerator to cool the samples down to  $5$  to  $6$  K minimum temperature. Similar to the IN3 experiment the crystals were mounted with the [001] axis vertical which results in a  $(hk0)$  horizontal scattering plane. The diffracted x-ray beam was collimated by  $20 \times 20 \text{ mm}^2$  slits in order to have a reasonable  $Q$  resolution of  $0.04$  rlu along [100] and [010]. We took data around the  $(4.5, 0.5, 0)$  superstructure position with typical counting times of  $1$  to  $2$  h per energy scan (from  $-10$  to  $25$  meV). All data points in the figures are drawn together with error bars denoting the  $\pm 1\sigma$  error given by the counting statistics or by the fits.

## III. RESULTS AND DISCUSSION

Figure 1(a) shows typical inelastic neutron-scattering scans in  $\text{Lu}(\text{Pt}_{0.6}\text{Pd}_{0.4})_2\text{In}$  at room temperature on IN3 along

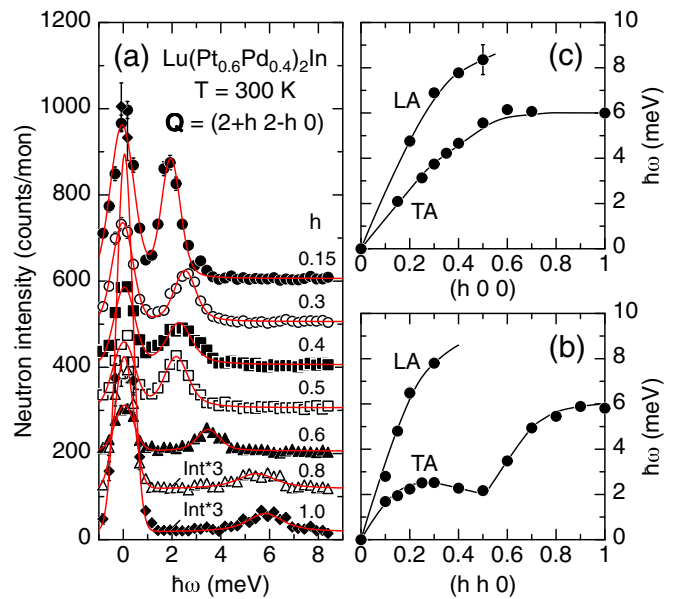


FIG. 1. (a) Energy scans in  $\text{Lu}(\text{Pt}_{0.6}\text{Pd}_{0.4})_2\text{In}$  measuring the lowest-lying acoustic phonons at different momentum transfer  $\mathbf{Q} = (2+h, 2-h, 0)$ . Data taken on IN3 at room temperature. Count rates for  $h = 0.8$  and  $1.0$  are enhanced by a factor of 3 and scans at different momentum transfer are shifted vertically with respect to each other for clarity. Solid lines are fits to the data consisting of an elastic line with Gaussian line shape and a Lorentzian peak shape for the inelastic phonons. (b) and (c) Phonon dispersions in  $\text{Lu}(\text{Pt}_{0.6}\text{Pd}_{0.4})_2\text{In}$  along the [110] and [100] directions at  $T = 300$  K showing TA and LA branches. Data indicate the phonon softening at  $\mathbf{q}_{\text{CDW}} = (0.5, 0.5, 0)$  for the TA branch. Solid lines are guides to the eyes.

$(2+h, 2-h, 0)$  measuring the acoustic phonons. We recorded data at various  $\mathbf{Q}$  positions to obtain the phonon dispersions along different directions. Both, the transverse and longitudinal acoustic (TA and LA, respectively) phonon branches for the [110] direction are shown in Fig. 1(b). Due to the experimental setup in our inelastic neutron and x-ray measurements we could only detect TA phonon branches along [110] with polarization along  $[1\bar{1}0]$ . Already at room temperature the softening has set in at  $\mathbf{q}_{\text{CDW}}$  in the TA phonon branch. The phonon dispersion along the [100] direction is displayed in Fig. 1(c). It does not show any softening and was more difficult to measure due to weaker phonon intensities and an uncertainty about the actual number of phonons at high energies. Therefore, especially above  $h = 0.5$ , the data are less reliable.

With the knowledge of the relevant phonon branch becoming soft, we started our measurements on a  $\text{Lu}(\text{Pt}_{0.5}\text{Pd}_{0.5})_2\text{In}$  single crystal using the high-resolution inelastic x-ray spectrometer BL35XU. To check the structural transition temperature we first measured on BL35XU the temperature dependence of the  $(4.5, 0.5, 0)$  superstructure intensity at zero energy transfer. Figure 2 displays the intensity versus temperature together with fits to the data. We detected no hysteresis in the data. The measurements indicate a continuous transition and broadly agree with x-ray results obtained previously [18], i.e., a strong increase of intensity to lower temperatures with

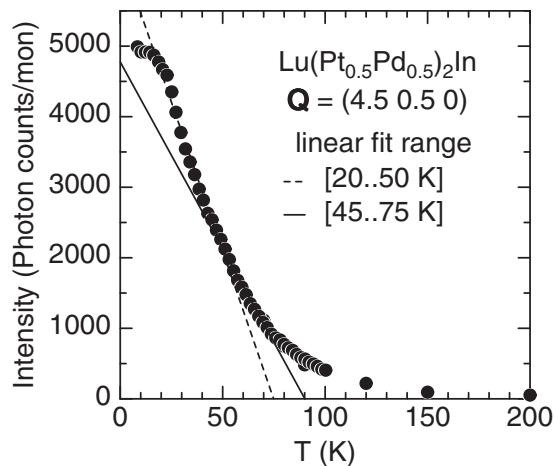


FIG. 2. Temperature dependence of the superstructure intensity in  $\text{Lu}(\text{Pt}_{0.5}\text{Pd}_{0.5})_2\text{In}$  at  $\mathbf{Q} = (4.5 \ 0.5 \ 0)$  measured on BL35XU.

a saturation only at lowest  $T$ . Since the absolute count rate in the detectors was low, a possible detector saturation due to extremely high count rates can be ruled out as origin of the unusual temperature dependence of the superstructure intensity. In contrast to the published data taken on powder samples [18], our measurement reveals a long tail of the intensity extending well above the transition temperature making the determination of the transition difficult. Such a behavior is likely due to enhanced structural fluctuations and points to their importance at the transition. Assuming a linear temperature dependence of the superstructure intensity as observed before [18] yields different transition temperatures  $T_{\text{CDW}}$  for the structural change depending on the fit range as can be seen by the solid and dashed lines in Fig. 2. Performing the fit between 20 and 50 K results in  $T_{\text{CDW}} = 75(1)$  K (the value in brackets denotes the  $1\text{-}\sigma$  error of the least-significant digits), whereas a fit range of 45–75 K gives  $T_{\text{CDW}} = 90(1)$  K. The latter value is in line with macroscopic measurements on polycrystalline  $\text{Lu}(\text{Pt}_{1-x}\text{Pd}_x)_2\text{In}$  [13], whereas the former is closer to the resistivity transitions in  $\text{Lu}(\text{Pt}_{0.5}\text{Pd}_{0.5})_2\text{In}$  single crystals [17] and to the powder x-ray diffraction results [18]. Certainly, the strong fluctuations do not allow to extract unambiguously the structural transition temperature in  $\text{Lu}(\text{Pt}_{0.5}\text{Pd}_{0.5})_2\text{In}$  in diffraction measurements. Similarly, tails in the superstructure intensity above  $T_{\text{CDW}}$  have recently been detected in  $\text{Ca}_3\text{Ir}_4\text{Sn}_{13}$  [18], but no or only very weak tails are present in  $\text{La}_3\text{Co}_4\text{Sn}_{13}$  [19],  $(\text{Ca}_{0.5}\text{Sr}_{0.5})_3\text{Rh}_4\text{Sn}_{13}$  [20],  $\text{Sr}_3\text{Ir}_4\text{Sn}_{13}$  [18], or the prototypical CDW-compounds  $\text{SrTiO}_3$ ,  $\text{EuTiO}_3$  [21], or  $2\text{H-NbSe}_2$  [22] rendering them more mean-field like.

We now turn to the inelastic x-ray measurements on  $\text{Lu}(\text{Pt}_{0.5}\text{Pd}_{0.5})_2\text{In}$  to study the low-energy phonons. Looking on the [110] direction we first show in Figs. 3(a) and 3(b) energy scans at 150 K and at different momentum transfers around (400) and (410). Due to an energy resolution being comparable to IN3 the low-energy phonons are well resolved on the energy-loss and the energy-gain side of the x-ray photons (for the fitting the detailed-balance factor for the phonons at positive/negative energies has been taken into account). From these measurements the phonon dispersion along [110] can be drawn and is displayed in Fig. 3(c). Together with the data for  $T = 150$  K also the results for  $T = 90$  and 250 K are

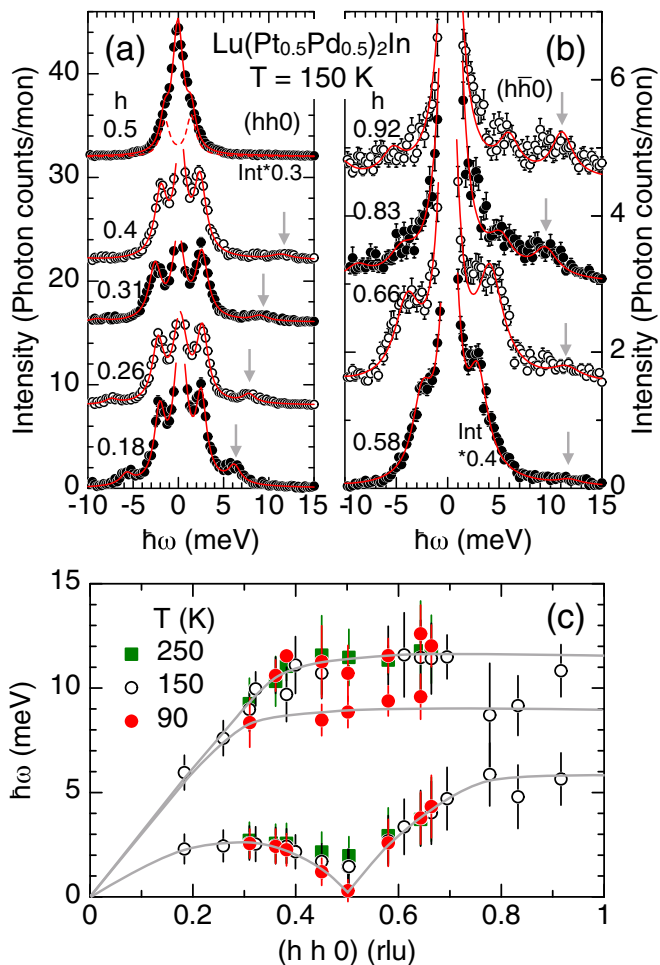


FIG. 3. (a) and (b) Energy scans in  $\text{Lu}(\text{Pt}_{0.5}\text{Pd}_{0.5})_2\text{In}$  at different momentum transfers at  $T = 150$  K to measure the dispersion along the [110] direction. (a) Scans for momentum transfer  $\mathbf{Q} = (400) + (hh0)$  and (b)  $\mathbf{Q} = (410) + (h\bar{h}0)$ . Solid lines indicate fits to the data being the sum of an elastic peak and inelastic peaks to model the phonons (with Lorentzian line shape). For  $h = 0.5$  the dashed line denotes the low-energy soft phonon. Arrows mark the higher-energy phonons. Individual scans in (a) and (b) are shifted vertically with respect to each other and intensities for  $h = 0.5$  and 0.58 are rescaled by 0.3 and 0.4, respectively. All data recorded on BL35XU. (c) Phonon dispersion along [110] in  $\text{Lu}(\text{Pt}_{0.5}\text{Pd}_{0.5})_2\text{In}$  at  $T = 150$  K [as a result of fits to the data shown in (a) and (b) and additional scans] and at  $T = 90$  and 250 K. Vertical bars denote the energy width of the phonons and not the error in the phonon energy. Solid lines are guides to the eyes. A clear phonon softening as function of temperature is visible at  $\mathbf{q}_{\text{CDW}} = (0.5 \ 0.5 \ 0)$  for the lowest-lying TA phonon branch.

shown. They are in line with the results for  $\text{Lu}(\text{Pt}_{0.6}\text{Pd}_{0.4})_2\text{In}$  obtained on IN3 [cf. Fig. 1(b)]. Whereas at higher energy the phonon branches remain unchanged at the different temperatures in  $\text{Lu}(\text{Pt}_{0.5}\text{Pd}_{0.5})_2\text{In}$ , a pronounced softening of the low-energy TA phonon branch around  $\mathbf{q}_{\text{CDW}} = (0.5 \ 0.5 \ 0)$  is seen when lowering the temperature. At 90 K an almost full phonon softening at (0.5 0.5 0) has taken place in  $\text{Lu}(\text{Pt}_{0.5}\text{Pd}_{0.5})_2\text{In}$ . Focusing on the soft phonon at (0.5 0.5 0), i.e., measuring at  $\mathbf{Q} = (4.5 \ 0.5 \ 0)$ , its temperature and mo-

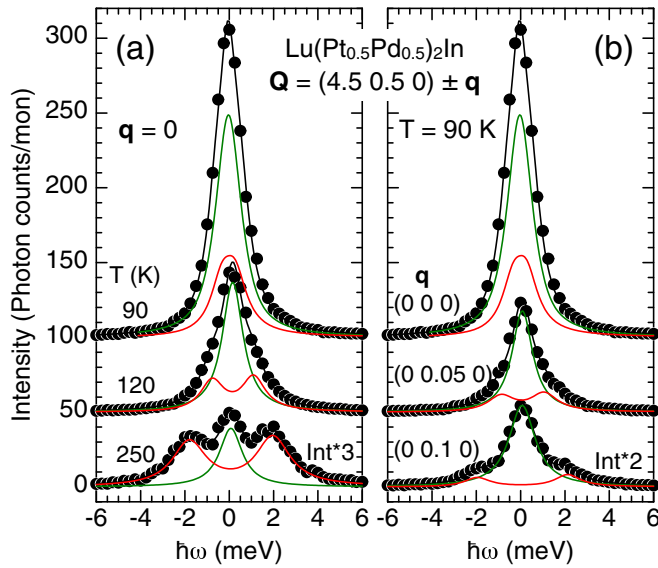


FIG. 4. (a) Energy scans in  $\text{Lu}(\text{Pt}_{0.5}\text{Pd}_{0.5})_2\text{In}$  at  $\mathbf{Q} = (4.5 \ 0.5 \ 0)$  at different temperatures. Solid lines are fits to the data (green lines: elastic signal, red lines: phonons, black lines: total fit of elastic signal and phonons). (b) Energy scans in  $\text{Lu}(\text{Pt}_{0.5}\text{Pd}_{0.5})_2\text{In}$  at  $\mathbf{Q} = (4.5 \ 0.5 \ 0) \pm \mathbf{q}$  at  $T = 90$  K. Solid lines are fits to the data (green lines: elastic signal, red lines: phonons, black lines: total fit of elastic signal and phonons). All data taken on BL35XU.

mentum dependence is presented in Figs. 4(a) and 4(b). The separation of the phonons (red lines) and the elastic contributions (green lines, due to critical scattering/superstructure and incoherent scattering) is only possible because of the very well-known energy resolution of the x-ray spectrometer. Increasing the temperature to well above the CDW transition or moving away from  $\mathbf{q}_{\text{CDW}} = (0.5 \ 0.5 \ 0)$  results in a strongly increased phonon energy. A full phonon softening only occurs at  $\mathbf{q}_{\text{CDW}}$  as can also be seen in Fig. 5. The further away from  $\mathbf{q}_{\text{CDW}}$ , the less temperature dependence of the phonon is observed. The smallest measured soft-phonon energies of well below 0.5 meV have to be taken with some caution because they are at the limit of what can be extracted from the x-ray data when deconvoluting with the instrumental resolution function with a width of roughly 1.4 meV. Within mean-field theory the soft phonon energy should depend on temperature as  $\hbar\omega_{\text{CDW}} \propto (T - T_{\text{CDW}})^{0.5}$  as already pointed out by Cochran [23]. Such a square-root temperature dependence of  $\omega_{\text{CDW}}$  broadly describes the softening as displayed by the red solid line in Fig. 5, but does not capture the region close to the transition. Whereas the fit yields a transition temperature of  $T_{\text{CDW}} = 76(8)$  K, visual inspection of the data (cf. Fig. 5) clearly indicates a transition temperature closer to 90 K. To better characterize the temperature dependence of the soft phonon more measurements closer, but also further away from the CDW transition are highly desired. Only then a probable non-mean-field behavior can be proven. The large tail in the superstructure intensity above the transition temperature (cf. Fig. 2) points to strong order-parameter fluctuations well above  $T_{\text{CDW}}$ . Hence, a deviation of the soft-phonon energy from mean-field behavior could well be expected. As seen in Fig. 5, even in  $\text{Lu}(\text{Pt}_{0.2}\text{Pd}_{0.8})_2\text{In}$ , i.e., above the critical Pd

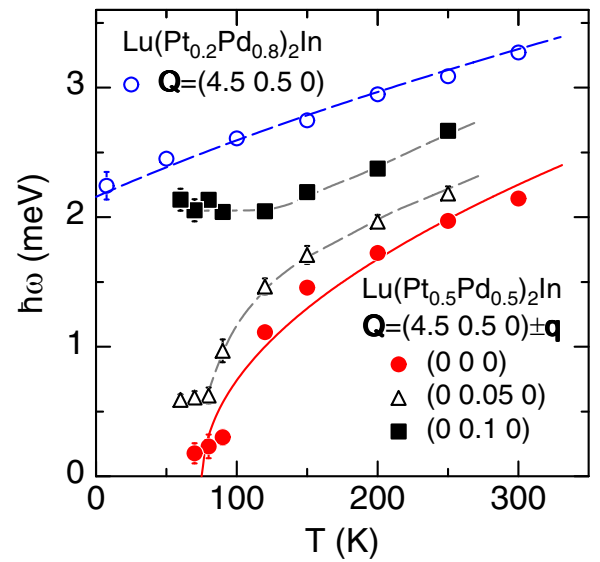


FIG. 5. Temperature dependence of the lowest-lying phonon energies in  $\text{Lu}(\text{Pt}_{0.5}\text{Pd}_{0.5})_2\text{In}$  in the vicinity of  $\mathbf{Q} = (4.5 \ 0.5 \ 0)$  along [010] and, for comparison, in  $\text{Lu}(\text{Pt}_{0.2}\text{Pd}_{0.8})_2\text{In}$  at  $\mathbf{Q} = (4.5 \ 0.5 \ 0)$ . Dashed lines are guides to the eye, whereas the solid line indicates a fit of the soft-phonon energy versus temperature assuming a mean-field behavior.

content  $x_c$  where no more a structural transition is present, the low-energy phonon at  $(0.5 \ 0.5 \ 0)$  shows some softening at low temperatures. It is currently open if and how such a partial phonon softening influences the low-temperature properties of  $\text{Lu}(\text{Pt}_{1-x}\text{Pd}_x)_2\text{In}$ . Here, the CDW transition and its disappearance at  $x_c$  has to be studied in more detail in the future.

In the following we briefly want to compare our experimental observations with predictions based on DFT calculations. A first DFT study of the phonons in  $\text{LuPt}_2\text{In}$  and  $\text{LuPd}_2\text{In}$  [13] indicated only positive phonon energies and gave, thus, no clear evidence for a structural instability. Only some limited phonon softening was predicted at  $\mathbf{q} = (100)$ , which was more pronounced for the Pt-based compound. Later on, Kim *et al.* [24] performed a calculation using an extended unit cell, and reported negative phonon energies around  $\mathbf{q} = (0.5 \ 0.5 \ 0)$  only for the Pt-based compound using the conventional notation for the fcc structure, indicating a structural instability in  $\text{LuPt}_2\text{In}$  with respect to this wave vector. Both DFT calculations [13,24] reproduce quite well the experimental sound velocities and their quite isotropic behavior along [100] and [110]. Whereas at first glance the calculations by Kim *et al.* [24] seem to confirm our observations, a more detailed comparison reveals marked differences. In  $\text{LuPt}_2\text{In}$  the calculated phonon energies of the lowest TA branch along [110] are negative from very small  $\mathbf{q}$  on, even in the limit for  $\mathbf{q} = 0$ . As a consequence, phonon softening is predicted in an extended  $\mathbf{q}$  range [ $0 \leq \mathbf{q} \lesssim (0.75 \ 0.75 \ 0)$ ] in strong contrast to our result where only a softening around  $\mathbf{q} = (0.5 \ 0.5 \ 0)$  is seen. Usually phonon softening in a CDW system occurs at a particular  $\mathbf{q}$  position (also in the “3-4-13” system mentioned below) and not in an extended  $\mathbf{q}$  range. A CDW instability and the connected phonon softening is

usually attributed to an enhanced electronic susceptibility at some specific momentum transfer in the reciprocal space, but an enhanced electron-phonon coupling is equally important, as, e.g., explicitly mentioned by Kim *et al.* [24]. For the present system they obtained a strongly enhanced susceptibility along [001] from (0.5 0.5 0) to (0.5 0.5 0.5), but at the end the electron phonon coupling being larger at (0.5 0.5 0) than at (0.5 0.5 0.5) is proposed to induce the instability at the former  $\mathbf{q}$  vector. Thus, along [110] the calculated electronic susceptibility has a sharp maximum at (0.5 0.5 0) which fits nicely to our observation that the softening occurs only close to (0.5 0.5 0). In general, whereas both published DFT calculations capture some basic phonon properties in LuPt<sub>2</sub>In, they are not able to correctly reproduce the observed phonon softening and the lattice instability. More advanced calculations taking into account long-range phononic interactions and correlations might be needed to correctly reproduce the observed lattice instability. Accordingly, it is presently difficult to assess how this phonon softening affects other low-temperature properties in this system.

At this point, we want to discuss our findings in comparison to results on the '3-4-13' family of cubic intermetallic compounds, in particular (Ca<sub>1-x</sub>Sr<sub>x</sub>)<sub>3</sub>Ir<sub>4</sub>Sn<sub>13</sub> [12,25,26]. The structural/CDW transition in this system can either be suppressed by applying hydrostatic pressure or by Ca substitution. For a critical Ca content  $x_c \approx 0.85$  a structural QCP is approached with a broad dome-like enhancement of superconductivity being present in (Ca<sub>1-x</sub>Sr<sub>x</sub>)<sub>3</sub>Ir<sub>4</sub>Sn<sub>13</sub> [12]. Despite marked differences in the high-temperature structure, a primitive cubic structure in the 3-4-13 compounds in comparison to a face-centered-cubic structure in our case of Lu(Pt<sub>1-x</sub>Pd<sub>x</sub>)<sub>2</sub>In, both families of compounds exhibit a body-centered-cubic structure at low temperatures, and a similar softening of the low-energy phonon at (0.5 0.5 0) [12,25,26]. The important question concerns the relation between the soft-phonon behavior and the enhancement of superconductivity

around the structural QCP. Whereas in the 3-4-13 system only a moderate enhancement of the superconducting  $T_c$  is visible, a much more pronounced superconducting dome is present in Lu(Pt<sub>1-x</sub>Pd<sub>x</sub>)<sub>2</sub>In around the structural QCP. One might speculate that the stronger order-parameter fluctuations in Lu(Pt<sub>1-x</sub>Pd<sub>x</sub>)<sub>2</sub>In as seen in the long tail of the superstructure intensity above  $T_{CDW}$  (cf. Fig. 2), are at the origin of the strong enhancement of the superconducting  $T_c$  around the QCP.

#### IV. CONCLUSIONS

To summarize, we performed extensive single-crystal inelastic neutron scattering and high-resolution inelastic x-ray scattering experiments on the cubic intermetallic system Lu(Pt<sub>1-x</sub>Pd<sub>x</sub>)<sub>2</sub>In to study the phonon softening associated with the structural transition. A full phonon softening is observed in Lu(Pt<sub>0.5</sub>Pd<sub>0.5</sub>)<sub>2</sub>In at  $\mathbf{q}_{CDW} = (0.5\ 0.5\ 0)$  with deviations from mean field behavior especially close to the structural/CDW transition  $T_{CDW}$ . The strong order-parameter fluctuations as inferred from the large tails in the superstructure intensity above  $T_{CDW}$  might be related to the pronounced enhancement of the superconducting  $T_c$  around the QCP in Lu(Pt<sub>1-x</sub>Pd<sub>x</sub>)<sub>2</sub>In.

#### ACKNOWLEDGMENTS

We greatly acknowledge helpful discussions with G. Fecher, F. Weber, M. Garst, M. Lang, and C. Krellner. For the inelastic neutron-scattering measurements we received technical help by M. Boehm and M. M. Koza. The neutron-scattering data are available in Ref. [27]. Support was provided by the Grants-in-Aid for Scientific Research (B) (Grant No. 19H04408) from the Japan Society of Promotion of Science. The x-ray measurements of this work were performed under the approval of JASRI (Proposals No. 2017A1295, No. 2017B1526, and No. 2017B1889).

- 
- [1] H. v. Löhneysen, A. Rosch, M. Vojta, and P. Wölfle, *Rev. Mod. Phys.* **79**, 1015 (2007).
  - [2] P. Gegenwart, Q. Si, and F. Steglich, *Nat. Phys.* **4**, 186 (2008).
  - [3] C. Pfleiderer, *Rev. Mod. Phys.* **81**, 1551 (2009).
  - [4] T. Shibauchi, A. Carrington, and Y. Matsuda, *Annu. Rev. Condens. Matter Phys.* **5**, 113 (2014).
  - [5] M. Brando, D. Belitz, F. M. Grosche, and T. R. Kirkpatrick, *Rev. Mod. Phys.* **88**, 025006 (2016).
  - [6] M. D. Johannes and I. I. Mazin, *Phys. Rev. B* **77**, 165135 (2008).
  - [7] G. Shirane, *Rev. Mod. Phys.* **46**, 437 (1974).
  - [8] R. A. Cowley and S. M. Shapiro, *J. Phys. Soc. Jpn.* **75**, 111001 (2006).
  - [9] L. E. Klintberg, S. K. Goh, P. L. Alireza, P. J. Saines, D. A. Tompsett, P. W. Logg, J. Yang, B. Chen, K. Yoshimura, and F. M. Grosche, *Phys. Rev. Lett.* **109**, 237008 (2012).
  - [10] Y. J. Hu, Y. W. Cheung, W. C. Yu, M. Imai, H. Kanagawa, J. Murakawa, K. Yoshimura, and S. K. Goh, *Phys. Rev. B* **95**, 155142 (2017).
  - [11] S. K. Goh, D. A. Tompsett, P. J. Saines, H. C. Chang, T. Matsumoto, M. Imai, K. Yoshimura, and F. M. Grosche, *Phys. Rev. Lett.* **114**, 097002 (2015).
  - [12] Y. W. Cheung, Y. J. Hu, M. Imai, Y. Tanioku, H. Kanagawa, J. Murakawa, K. Moriyama, W. Zhang, K. T. Lai, K. Yoshimura, F. M. Grosche, K. Kaneko, S. Tsutsui, and S. K. Goh, *Phys. Rev. B* **98**, 161103(R) (2018).
  - [13] T. Gruner, D. Jang, Z. Huesges, R. Cardoso-Gil, G. H. Fecher, M. M. Koza, O. Stockert, A. P. Mackenzie, M. Brando, and C. Geibel, *Nat. Phys.* **13**, 967 (2017).
  - [14] T. Gruner, D. Jang, A. Steppke, M. Brando, F. Ritter, C. Krellner, and C. Geibel, *J. Phys.: Condens. Matter* **26**, 485002 (2014).
  - [15] H. Kim, J. H. Shim, S. Kim, J.-H. Park, K. Kim, and B. I. Min, *Phys. Rev. Lett.* **125**, 157001 (2020).
  - [16] M. O. Ajeesh, T. Gruner, C. Geibel, and M. Nicklas, *J. Phys. Soc. Jpn.* **90**, 035001 (2021).
  - [17] T. Gruner, S. A. Hodgson, C. Geibel, O. Stockert, and F. M. Grosche, *J. Phys. Soc. Jpn.* **90**, 064706 (2021).
  - [18] F. B. Carneiro, L. S. I. Veiga, J. R. L. Mardegan, R. Khan, C. Macchiutti, A. López, and E. M. Bittar, *Phys. Rev. B* **101**, 195135 (2020).
  - [19] Y. W. Cheung, J. Z. Zhang, J. Y. Zhu, W. C. Yu, Y. J. Hu, D. G. Wang, Y. Otomo, K. Iwasa, K. Kaneko, M. Imai, H. Kanagawa,

- K. Yoshimura, and S. K. Goh, *Phys. Rev. B* **93**, 241112(R) (2016).
- [20] Y. W. Cheung, Y. J. Hu, S. K. Goh, K. Kaneko, S. Tsutsui, P. W. Logg, F. M. Grosche, H. Kanagawa, Y. Tanioku, M. Imai, T. Matsumoto, and K. Yoshimura, *J. Phys.: Conf. Ser.* **807**, 032002 (2017).
- [21] D. S. Ellis, H. Uchiyama, S. Tsutsui, K. Sugimoto, K. Kato, D. Ishikawa, and A. Q. R. Baron, *Phys. Rev. B* **86**, 220301(R) (2012).
- [22] F. Weber, S. Rosenkranz, J.-P. Castellan, R. Osborn, R. Hott, R. Heid, K.-P. Bohnen, T. Egami, A. H. Said, and D. Reznik, *Phys. Rev. Lett.* **107**, 107403 (2011).
- [23] W. Cochran, *Adv. Phys.* **9**, 387 (1960).
- [24] H. Kim, B. I. Min, and K. Kim, *Phys. Rev. B* **98**, 144305 (2018).
- [25] D. G. Mazzone, S. Gerber, J. L. Gavilano, R. Sibille, M. Medarde, B. Delley, M. Ramakrishnan, M. Neugebauer, L. P. Regnault, D. Chernyshov, A. Piovano, T. M. Fernández-Díaz, L. Keller, A. Cervellino, E. Pomjakushina, K. Conder, and M. Kenzelmann, *Phys. Rev. B* **92**, 024101 (2015).
- [26] K. Kaneko, Y. W. Cheung, Y. Hu, M. Imai, Y. Tanioku, H. Kanagawa, J. Murakawa, K. Moriyama, W. Zhang, K. T. Lai, M. Matsuda, K. Yoshimura, S. Tsutsui, and S. K. Goh, *JPS Conf. Proc.* **30**, 011032 (2020).
- [27] S. Lucas, M. Boehm, C. Geibel, T. Gruner, M. M. Koza, O. Stockert, Institut Laue-Langevin (2017), doi: [10.5291/ILL-DATA.7-02-165](https://doi.org/10.5291/ILL-DATA.7-02-165).